Test-particle diffusion in synthetic turbulent magnetic fields

Oreste Pezzi

oreste.pezzi@gssi.it www.orestepezzi.org

A. Dundovic, C. Evoli, W.H. Matthaeus and P. Blasi

GRAN SASSO SCIENCE INSTITUTE
SCHOOL OF ADVANCED STUDIES
Scuola Universitaria Superiore

University of Delaware

Cosmic Ray Anisotropy Workshop CRA2019
L'Aquila - 7-11 October 2019

Abstract

- **Introduction**

- **Numerical methods**
  - **Test-particle code**
  - **Synthetic model of the field**

- **Numerical Results**
  - **Case without B_0**
  - **Case with B_0**

- **Conclusions and perspectives**

Introduction

Propagation of galactic CRs (E ~ 10^{15} -10^{16} eV) in the interstellar medium:

- **Solution of the transport equation for CRs:**

$$\frac{\partial f}{\partial t} - \frac{\partial}{\partial z}\left(D_{zz}\frac{\partial f}{\partial z}\right) + v_A\frac{\partial f}{\partial z} - \frac{dv_A}{dz}\frac{p}{3}\frac{\partial f}{\partial p} + \frac{1}{p^2}\frac{\partial}{\partial p}\left[p^2\left(\frac{dp}{dt}\right)_{\rm ion} f\right] = Q_{\rm CR},$$

  - **No dynamical constraint due to computational limits**
  - **Nonlinear effects: self-confinement** (Kulsrud and Pierce, 1969, …, Evoli et al. 2018)
  - **Diffusion coefficient is based on “questionable” CRs transport theories**

- **Numerical modeling of CRs in a synthetic turbulent field:**
  - **Dynamical range is limited by computational power**
  - **Insights to develop better theory**

- **Numerical modeling of CRs in a MHD turbulent field:**
  - **Dynamical range is limited by computational power**
  - **Role of electric field and reconnecting islands for accelerating particles**

Test-particle code

Motion equations are numerically solved for N particles:

$$\frac{d\boldsymbol{r}}{dt} = \boldsymbol{v}$$

$$\frac{d\boldsymbol{u}}{dt} = \frac{q}{m}\left(\boldsymbol{E} + \frac{\boldsymbol{v}}{c} \times \boldsymbol{B}\right)$$

$$\boldsymbol{u} = \boldsymbol{p}/m = \gamma \boldsymbol{v},$$

$$\gamma = 1/\sqrt{1 - v^2/c^2} = \sqrt{1 + u^2/c^2}$$

Test-particle code

Motion equations are numerically solved for N particles:

$$\frac{d\boldsymbol{r}}{dt} = \boldsymbol{v}$$

$$\frac{d\boldsymbol{u}}{dt} = \frac{q}{m}\left(\boldsymbol{E} + \frac{\boldsymbol{v}}{c} \times \boldsymbol{B}\right)$$

$$\boldsymbol{u} = \boldsymbol{p}/m = \gamma \boldsymbol{v},$$

$$\gamma = 1/\sqrt{1 - v^2/c^2} = \sqrt{1 + u^2/c^2}$$

- **Two different orbit integrators:**
  - Boris scheme
  - Adaptive Runge-Kutta method with the Cash-Karp coefficients

Test-particle code

Motion equations are numerically solved for N particles:

$$\frac{d\boldsymbol{r}}{dt} = \boldsymbol{v}$$

$$\frac{d\boldsymbol{u}}{dt} = \frac{q}{m}\left(\boldsymbol{E} + \frac{\boldsymbol{v}}{c} \times \boldsymbol{B}\right)$$

$$\boldsymbol{u} = \boldsymbol{p}/m = \gamma \boldsymbol{v},$$

$$\gamma = 1/\sqrt{1 - v^2/c^2} = \sqrt{1 + u^2/c^2}$$

- **Two different orbit integrators:**
  - Boris scheme
  - Adaptive Runge-Kutta method with the Cash-Karp coefficients
- **Magnetic Field**
  - Defined on a [N_x, N_y ,N_z] uniform grid, with periodic BC **(FFT)**
  - Trilinear method or cubic splines to interpolate **B** at each particle position

Test-particle code

Motion equations are numerically solved for N particles:

$$\frac{d\boldsymbol{r}}{dt} = \boldsymbol{v}$$

$$\frac{d\boldsymbol{u}}{dt} = \frac{q}{m}\left(\boldsymbol{E} + \frac{\boldsymbol{v}}{c} \times \boldsymbol{B}\right)$$

$$\boldsymbol{u} = \boldsymbol{p}/m = \gamma \boldsymbol{v},$$

$$\gamma = 1/\sqrt{1 - v^2/c^2} = \sqrt{1 + u^2/c^2}$$

- **Two different orbit integrators:**
  - Boris scheme
  - Adaptive Runge-Kutta method with the Cash-Karp coefficients
- **Magnetic Field**
  - Defined on a [N_x, N_y ,N_z] uniform grid, with periodic BC **(FFT)**
  - Trilinear method or cubic splines to interpolate **B** at each particle position
- **Particles Injection:**
  - Random position;
  - Constant energy and isotropic in μ and θ.

Two different implementations

Synthetic model of the turbulent field

$$B = B_0 + \delta B$$

Turbulent perturbation:

- Isotropic energy spectrum with Kolmogorov slope (Γ= 5/3)
- Random phase;
- Bendover scale λ to mimic injection of turbulent fluctuations:

S(k) ~ k² at low wavenumber

Background field, along z

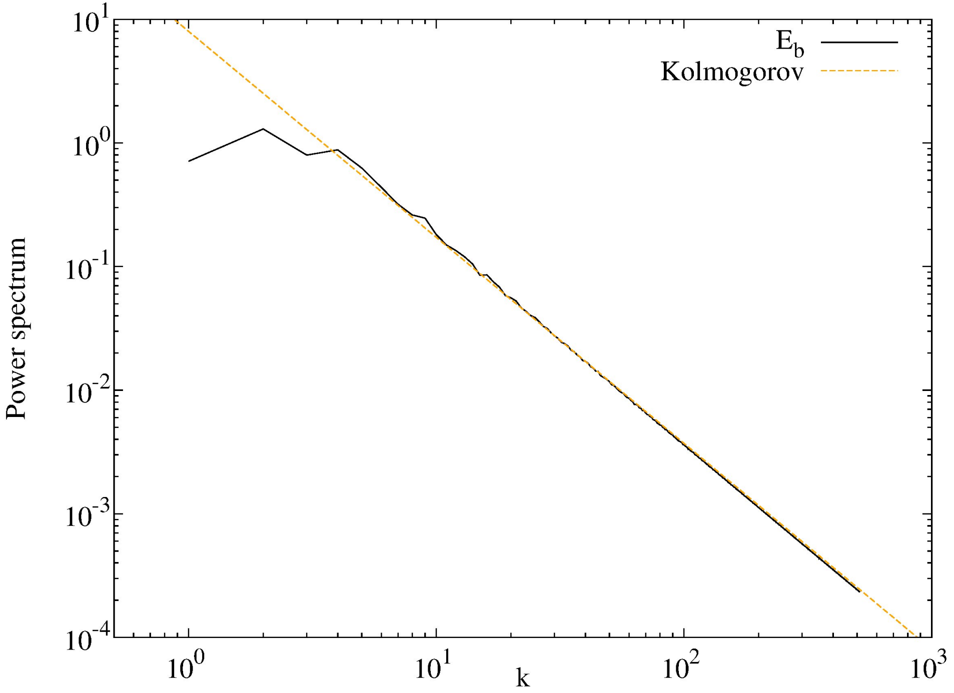

$$\mathbf{b}(\mathbf{k}) = \frac{1}{2}\sqrt{S(k)}\left[\mathbf{b}_1(\mathbf{k})e^{i\phi_1(\mathbf{k})} + i\mathbf{b}_2(\mathbf{k})e^{i\phi_2(\mathbf{k})}\right]$$

$$S(k) = C\frac{k^2\lambda^2}{\left(1 + k^2\lambda^2\right)^{\Gamma/2+2}}$$

(Sonsrettee et al., APJ, 2015)

Synthetic model of the turbulent field

$$B = B_0 + \delta B$$

Turbulent perturbation:

- Isotropic energy spectrum with Kolmogorov slope (Γ= 5/3)
- Random phase;
- Bendover scale λ to mimic injection of turbulent fluctuations:

  S(k) ~ k² at low wavenumber

Background field, along z

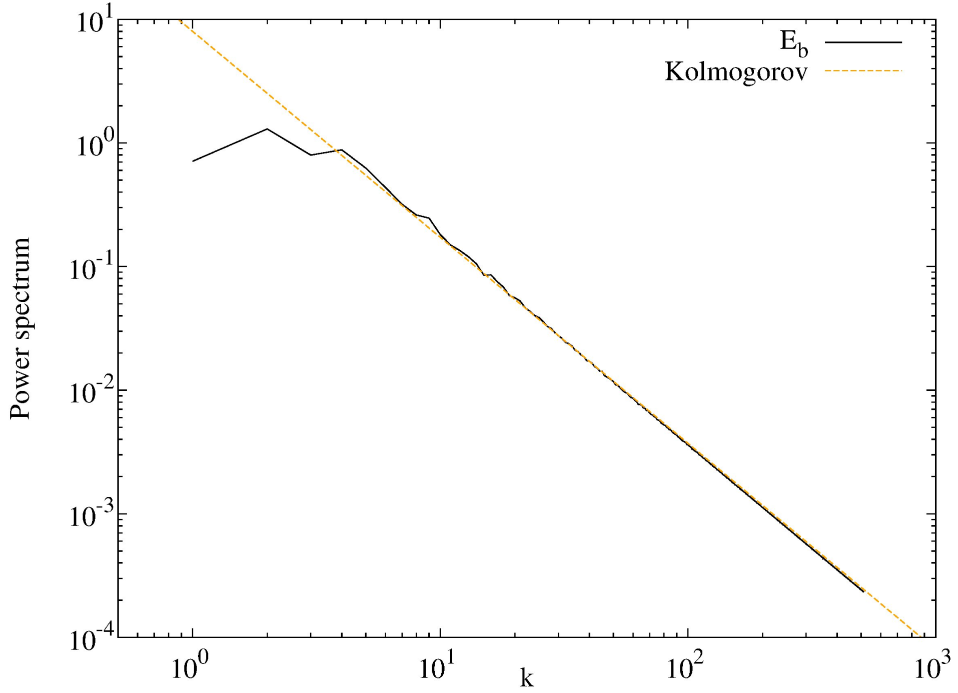

$$\mathbf{b}(\mathbf{k}) = \frac{1}{2}\sqrt{S(k)}\left[\mathbf{b}_1(\mathbf{k})e^{i\phi_1(\mathbf{k})} + i\mathbf{b}_2(\mathbf{k})e^{i\phi_2(\mathbf{k})}\right]$$

$$S(k) = C\frac{k^2\lambda^2}{\left(1 + k^2\lambda^2\right)^{\Gamma/2+2}}$$

(Sonsrettee et al., APJ, 2015)

$N_x = N_y = N_z = 1024$

$\lambda = L_{box} / 8$

$l_c \sim L_{box} / 16$

$B_0 = 1\ \mu G$

$l_c \sim 30$ pc

Numerical results: case without B_0

$B_0 = 0$

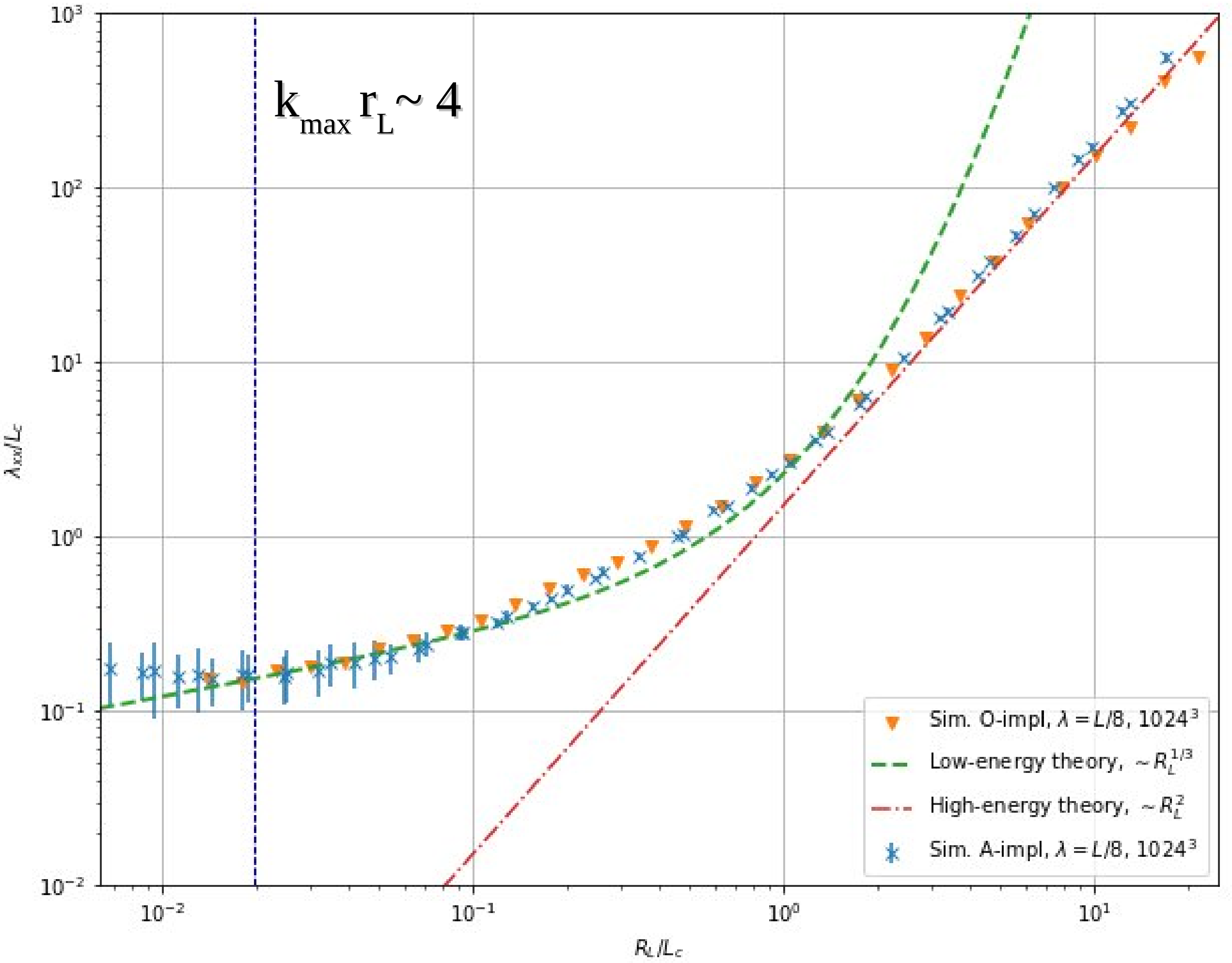

Numerical results: case without B_0

$B_0 = 0$

High-energy theory $r_L/l_c \gg 1$:

- Several uncorrelated fields within a gyration;
- Small particle deflections due to magnetic field irregularities;
- Diffusion achieved when δB is uncorrelated.

$$\kappa_{xx} = \kappa_{yy} = \kappa_{zz} = \frac{v^3}{2\Omega_0^2 l_c} \sim r_L^{\,2}$$

Aloisio & Berezinsky, 2004
Subedi et al., 2017

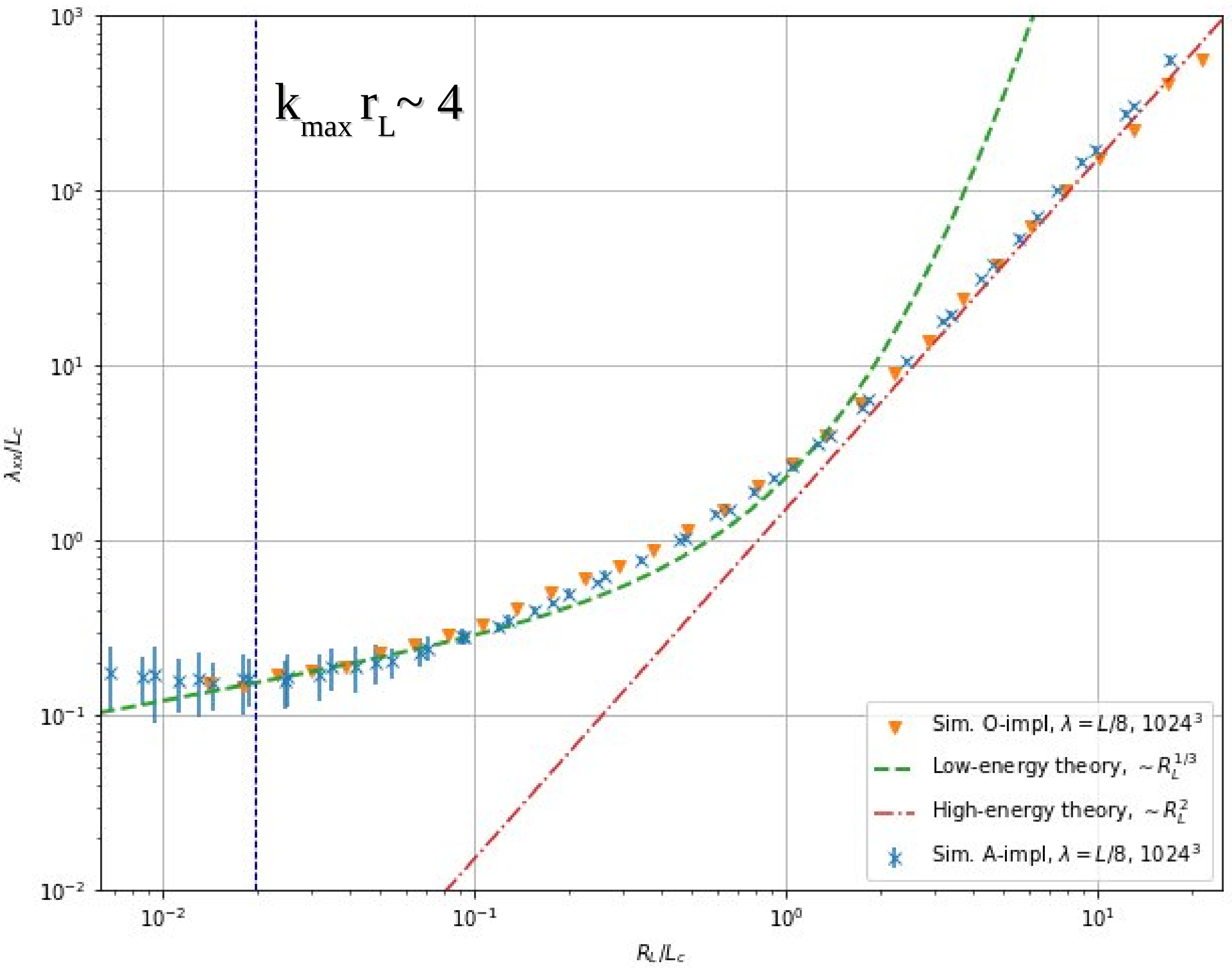

Numerical results: case without B_0

$B_0 = 0$

Low-energy theory $r_L/l_c \ll 1$:

- Particles experience the presence of a local coherent field, due to large-scale fluctuations (l_c)
- Two dominant effects:
  - Field line random walk
  - Resonant wave particle scattering
    $k \sim 1/r_L$

$$\kappa_{xx} = \kappa_{yy} = \kappa_{zz} = \kappa_{\|}/3$$

$$\kappa_{\|} = \frac{v^2}{8} \int_{-1}^{1} d\mu \, \frac{(1-\mu^2)^2}{D_{\mu\mu}}$$

Subedi et al., 2017

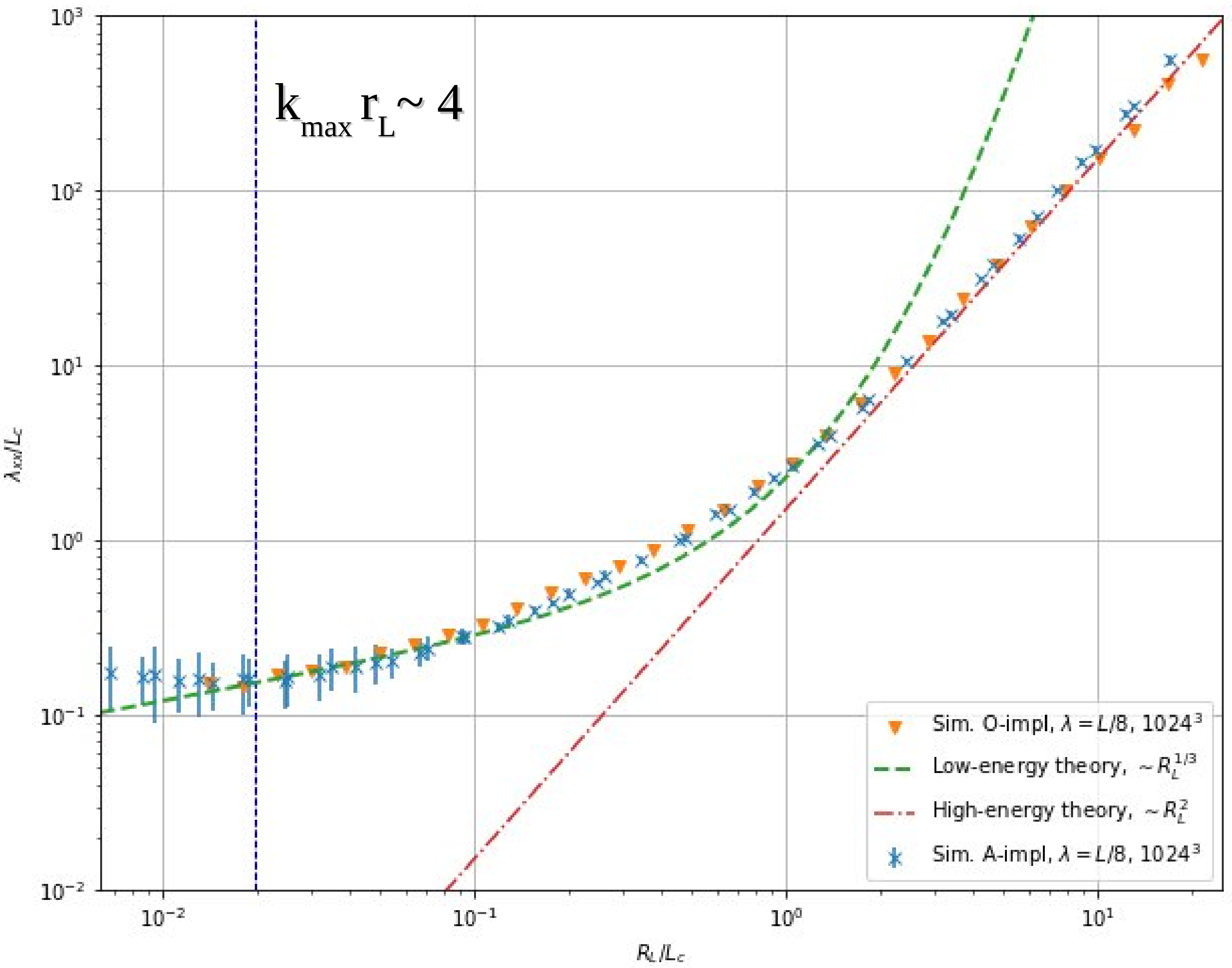

Numerical results: case without B_0

$B_0 = 0$

Low-energy theory $r_L/l_c << 1$:

- Particles experience the presence of a local coherent field, due to large-scale fluctuations (l_c)
- Two dominant effects:
  - Field line random walk
  - Resonant wave particle scattering
    $k \sim 1/r_L$

$$\kappa_{xx} = \kappa_{yy} = \kappa_{zz} = \kappa_{\|}/3$$

$$\kappa_{\|} = \frac{v^2}{8}\int_{-1}^{1} d\mu \, \frac{(1-\mu^2)^2}{D_{\mu\mu}}$$

$r_L^{1/3}$ slope

Correct normalization

Subedi et al., 2017

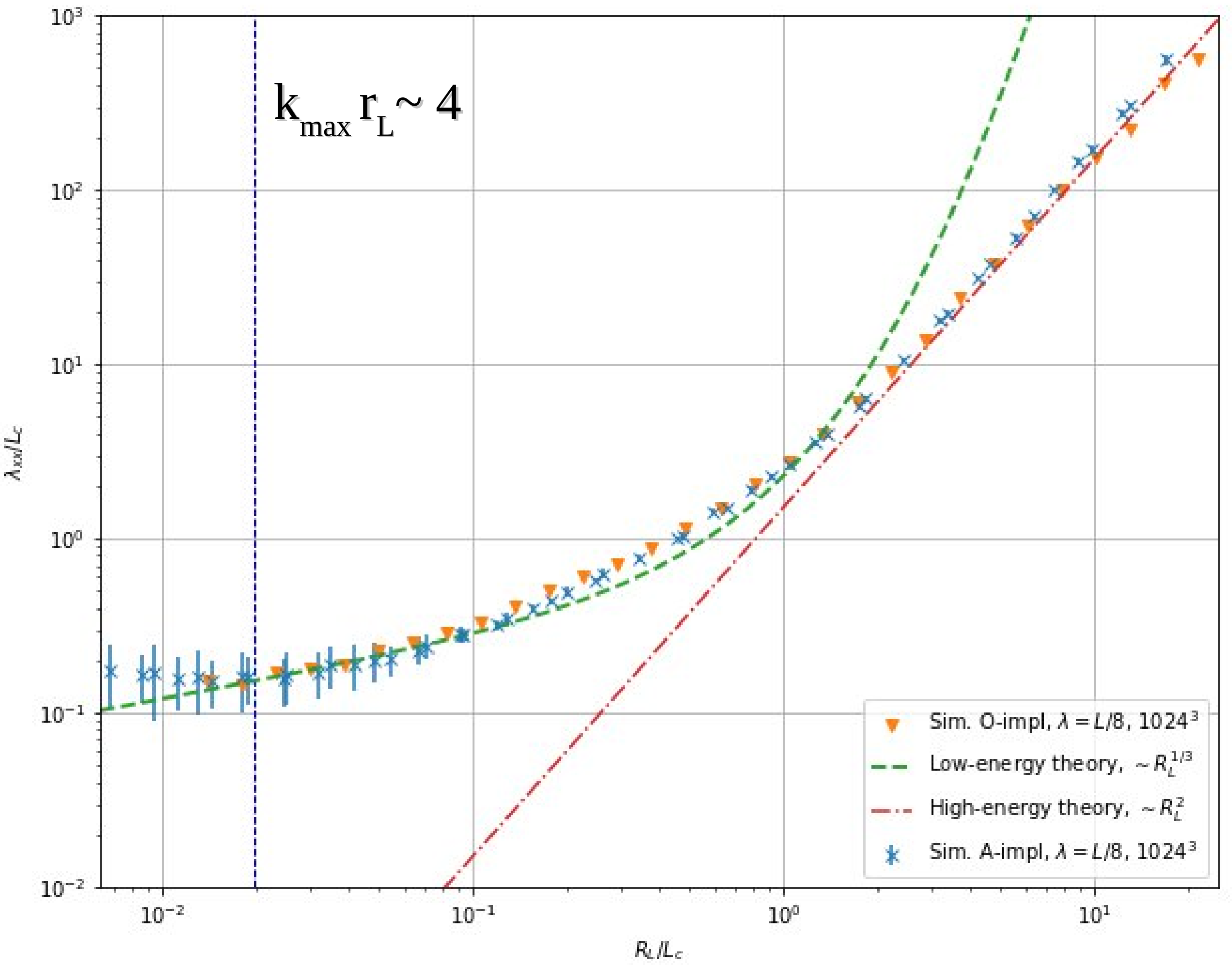

Numerical results: case with B_0

$\delta B_{rms}/B_0 = 2$

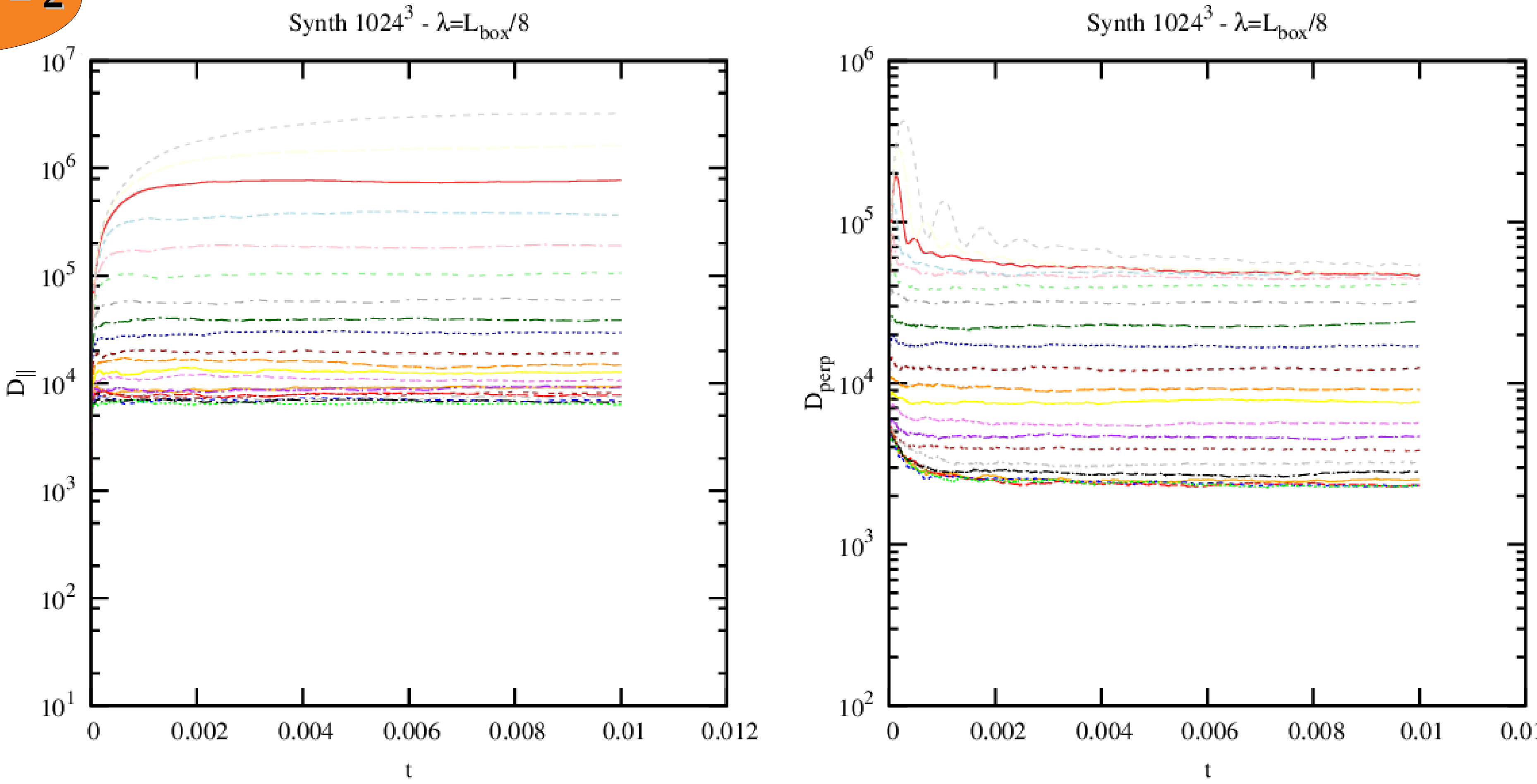

Numerical results: case with B_0

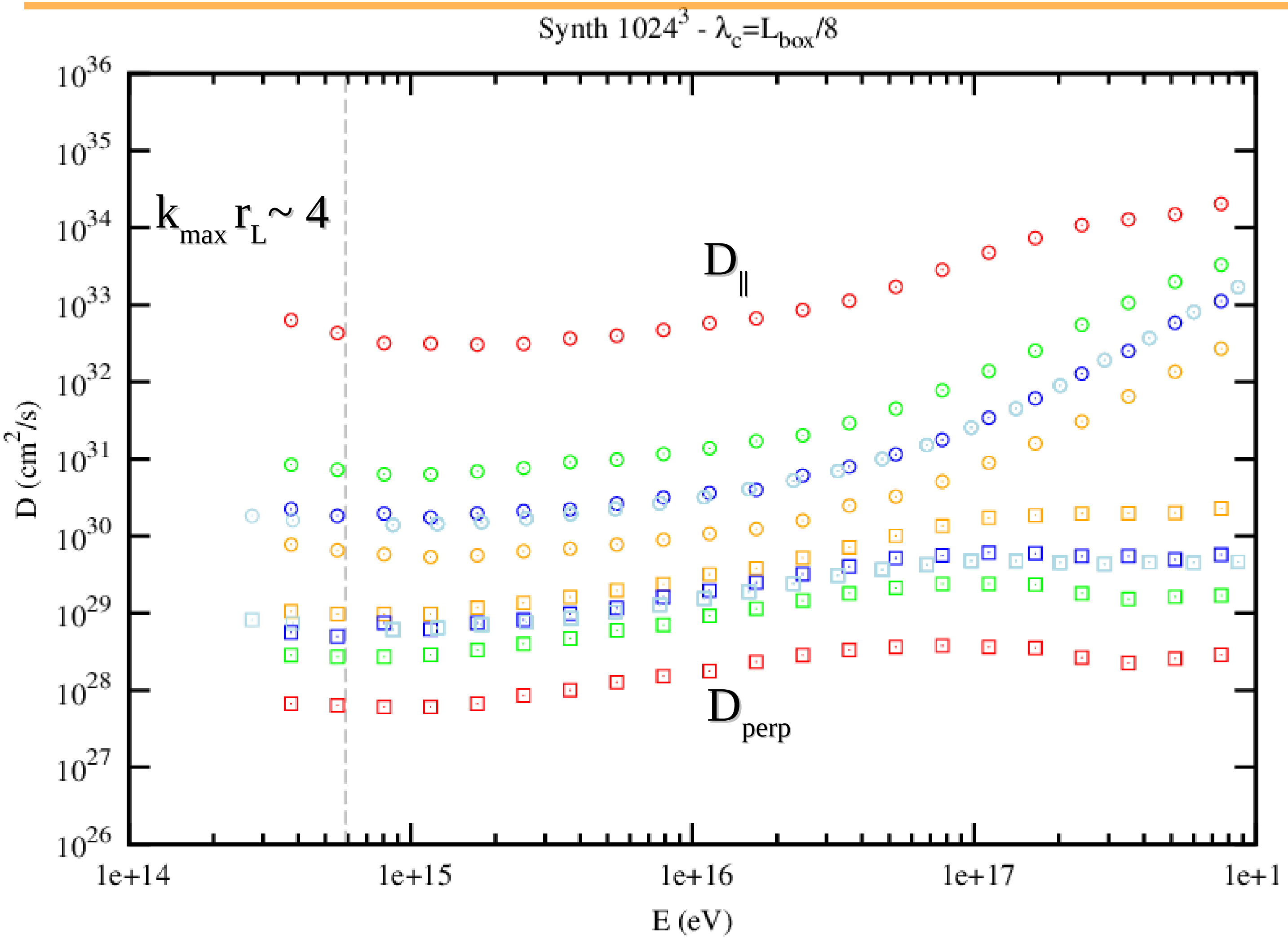

$\delta B_{rms}/B_0$ = 0.1

$\delta B_{rms}/B_0$ = 0.5

$\delta B_{rms}/B_0$ = 1

$\delta B_{rms}/B_0$ = 2

Case with B_0: parallel diffusion

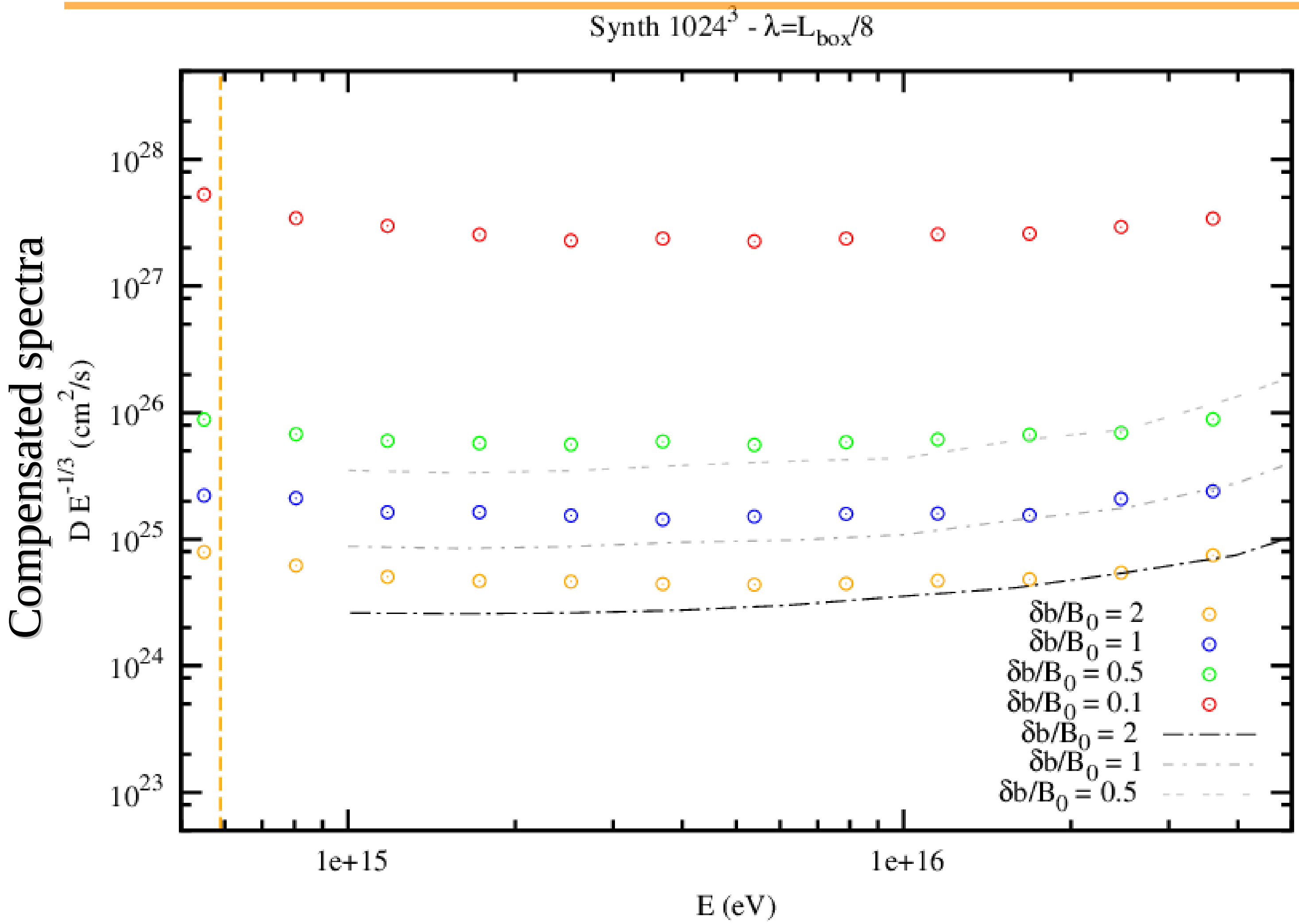

Dynamical range much more extended with respect to previous works

(De Marco and Blasi, 2007)

Case with B_0: perpendicular diffusion

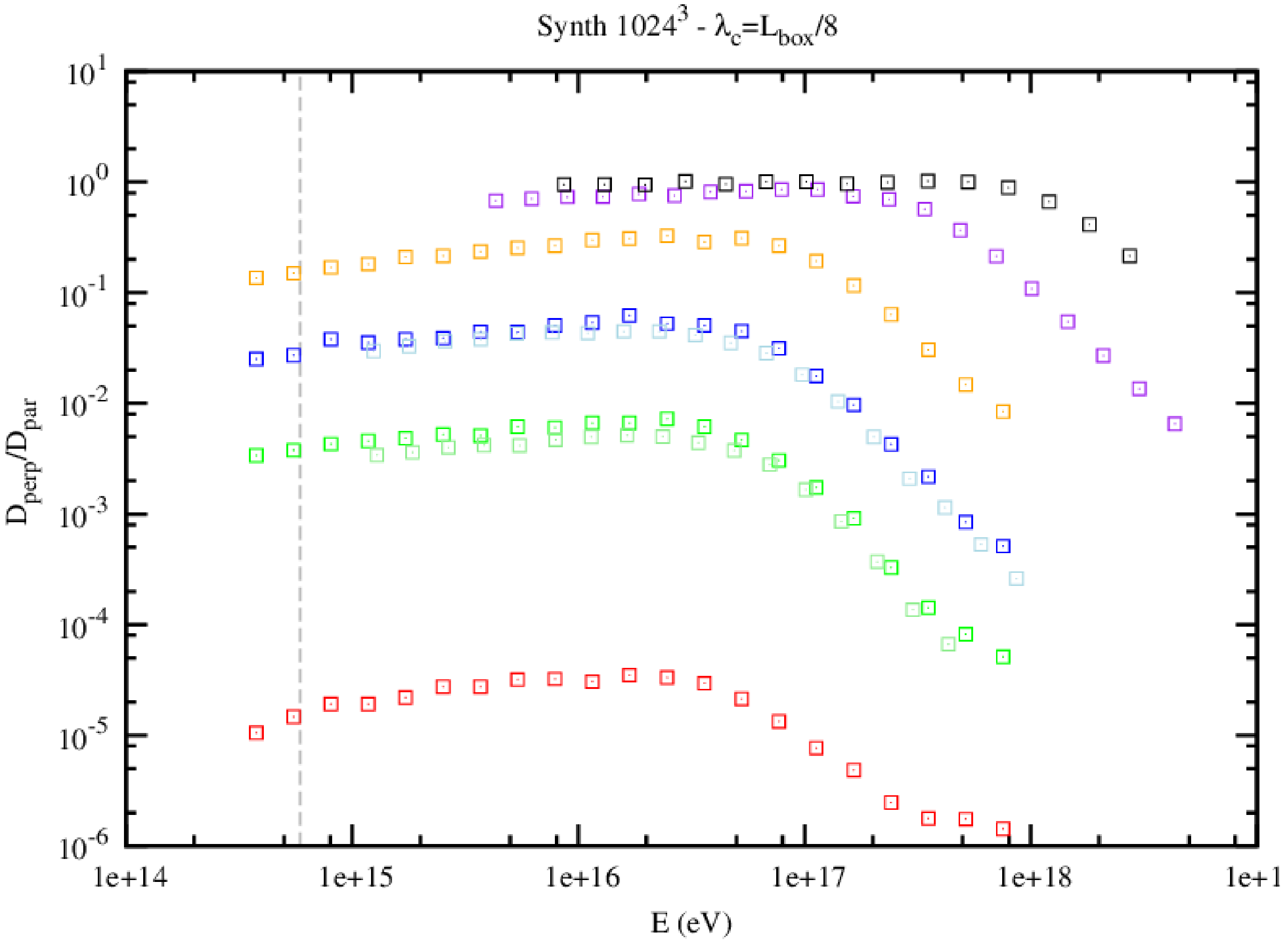

$\delta B_{rms}/B_0 = 0.1$

$\delta B_{rms}/B_0 = 0.5$

$\delta B_{rms}/B_0 = 1$

$\delta B_{rms}/B_0 = 2$

$\delta B_{rms}/B_0 = 5$

$\delta B_{rms}/B_0 = 10$

Case with B_0: perpendicular diffusion

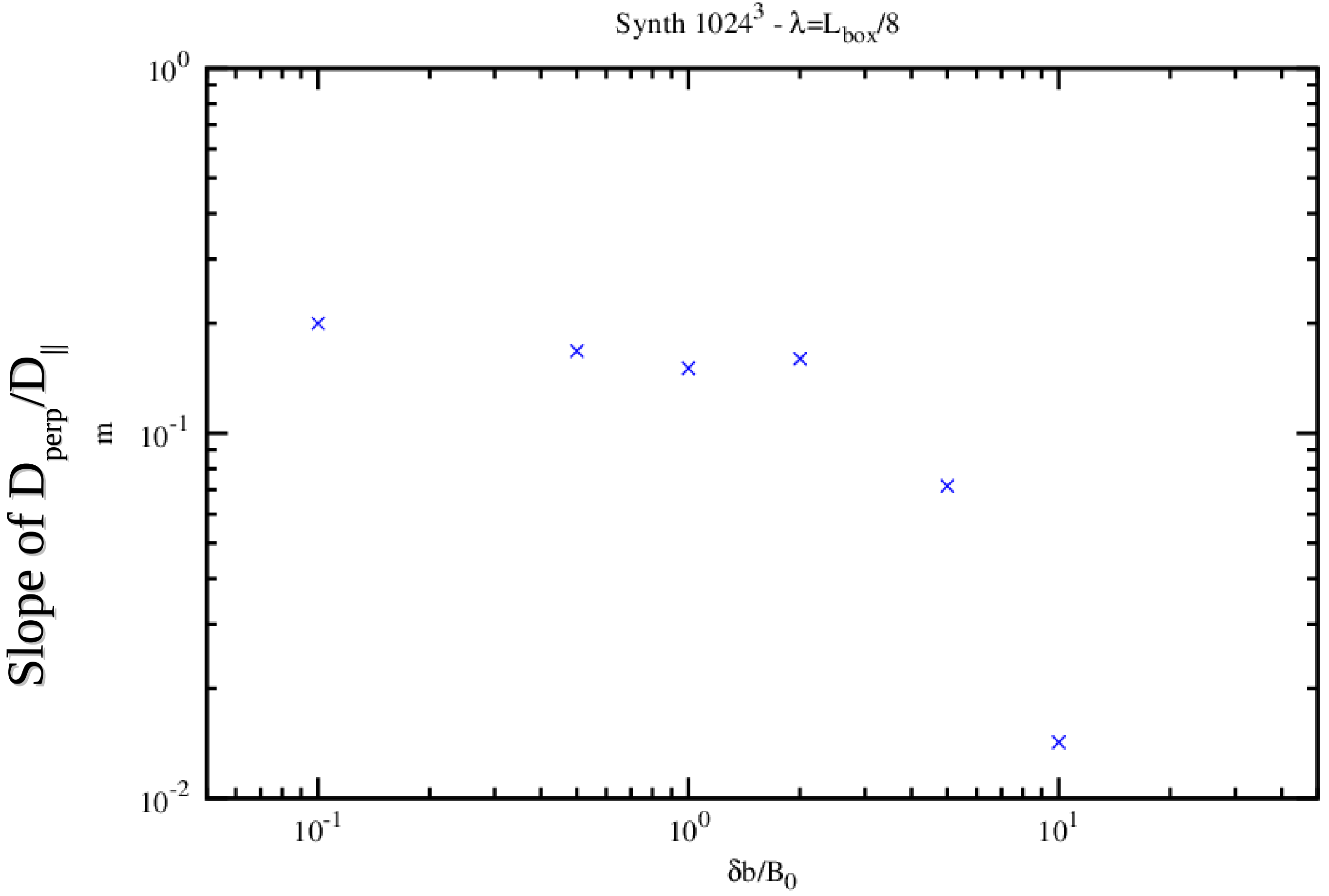

Different slopes…

… asymptotically:

$\mathbf{D_{\|} \sim E^{1/3}}$

$\mathbf{D_{perp} \sim E^{0.5}}$ **(?)**

Case with B_0: theoretical needs

NLGC as well as further “universal” theories predict that **$D_{||}$ and D_{perp} are parallel**.

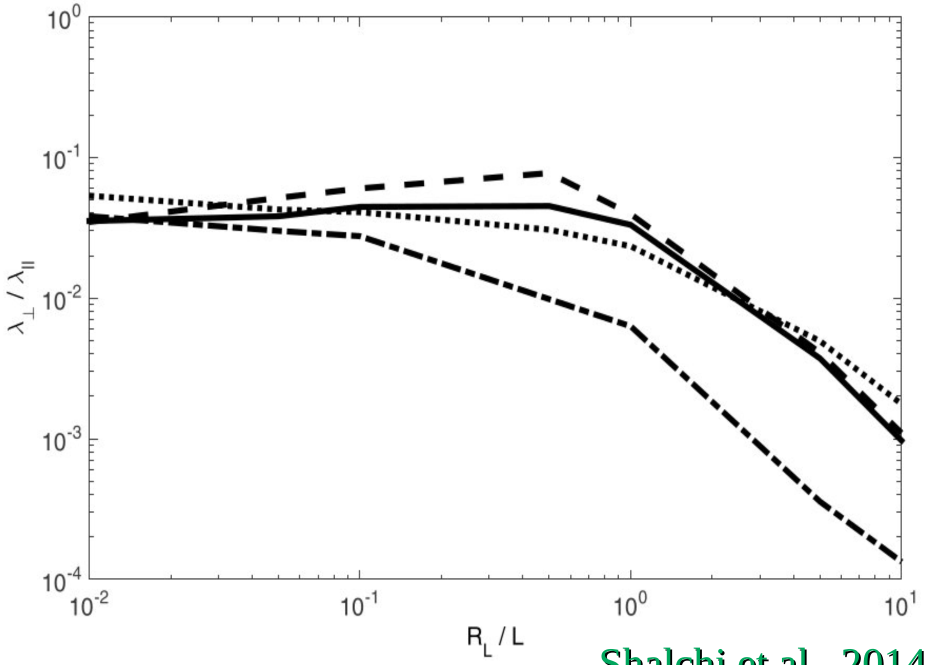

Shalchi et al., 2014
Hussein et al., 2015

Case with B_0: theoretical needs

NLGC as well as further “universal” theories predict that **$D_{||}$ and D_{perp} are parallel**.

Numerical simulations were actually indicating a **different behavior**!

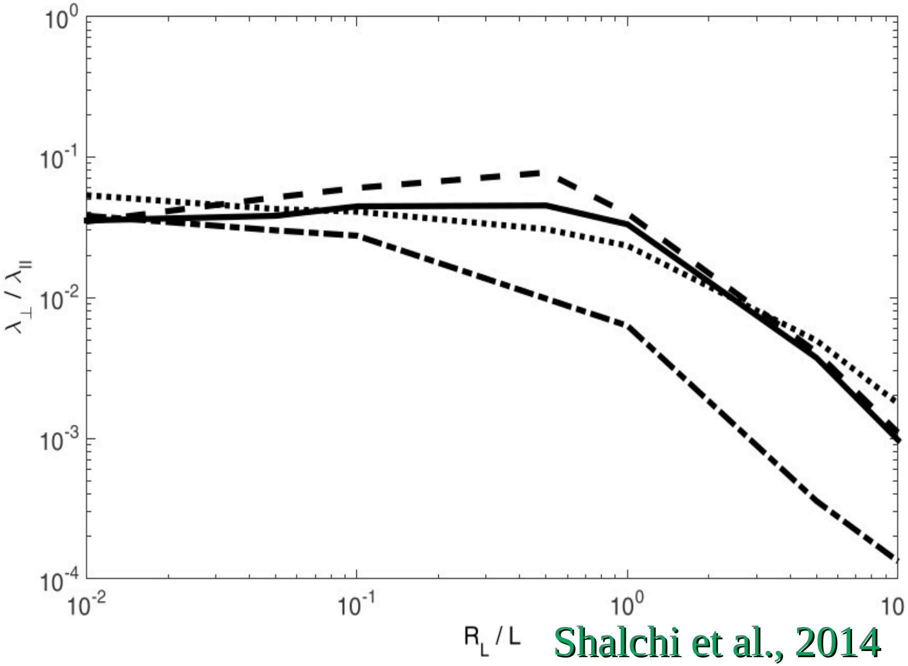

Shalchi et al., 2014
Hussein et al., 2015

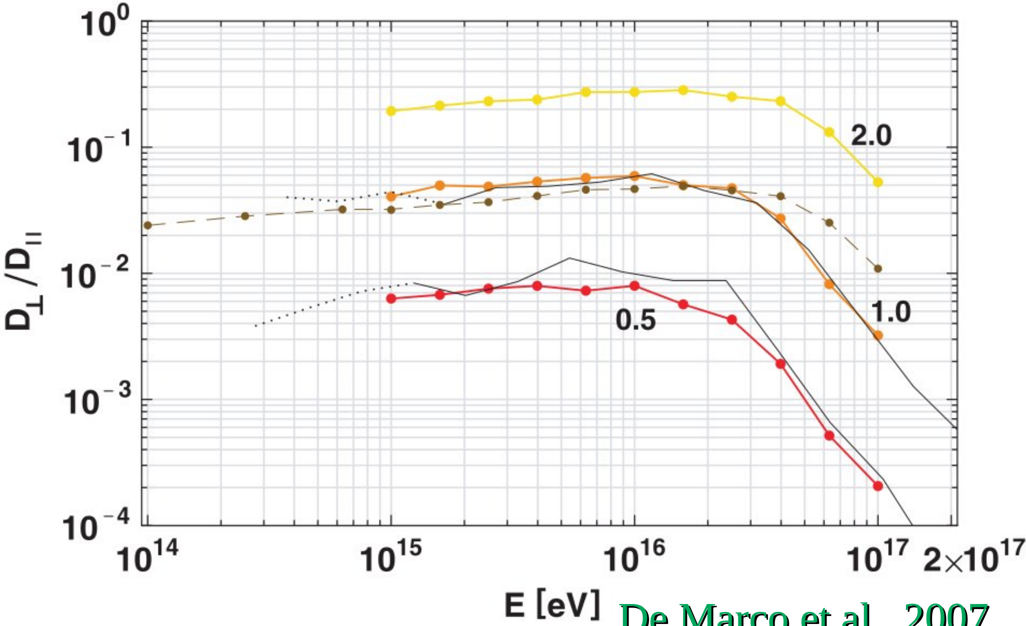

De Marco et al., 2007
Giacinti et al., 2018

Case with B_0: theoretical needs

NLGC as well as further "universal" theories predict that **$D_{||}$ and D_{perp} are parallel**.

Numerical simulations were actually indicating a **different behavior**!

We can provide now a better evidence of such behavior (grid up to 2048^3)

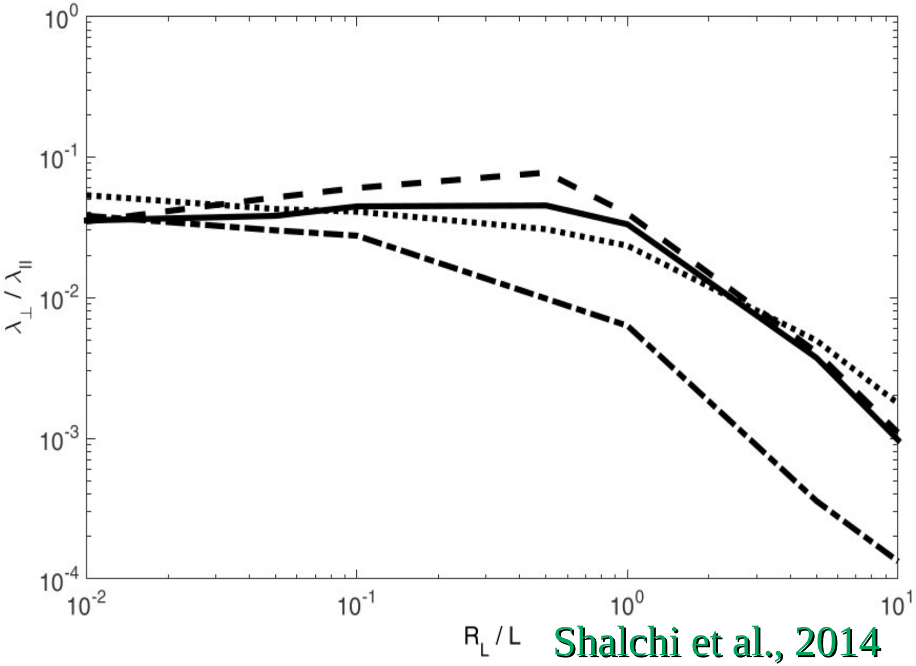

Shalchi et al., 2014

Hussein et al., 2015

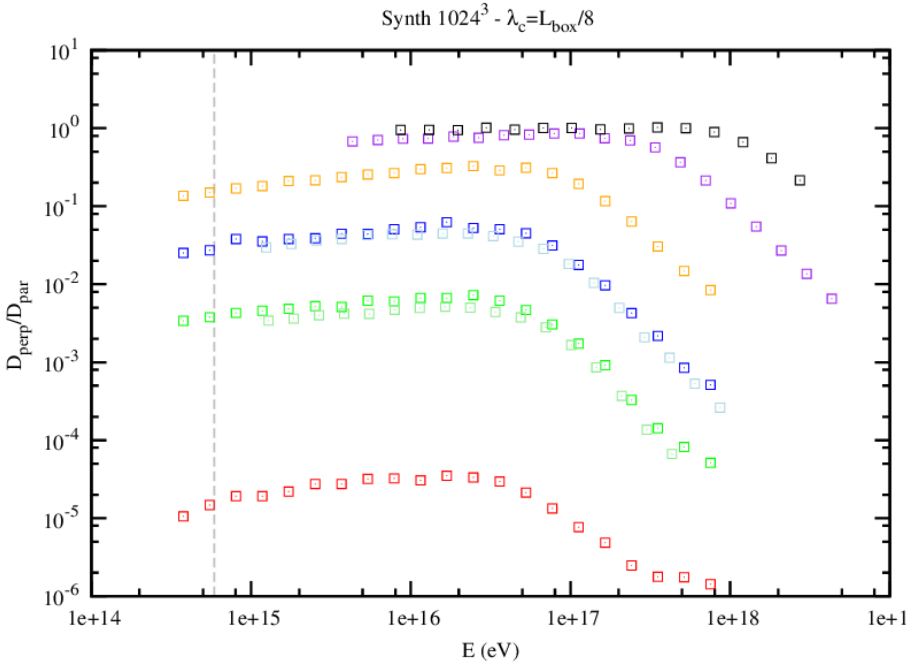

Case with B_0: theoretical needs

NLGC as well as further “universal” theories predict that **$D_{||}$ and D_{perp} are parallel**.

Numerical simulations were actually indicating a **different behavior**!

We can provide now a better evidence of such behavior (grid up to 2048^3)

Theory needs to be revisited

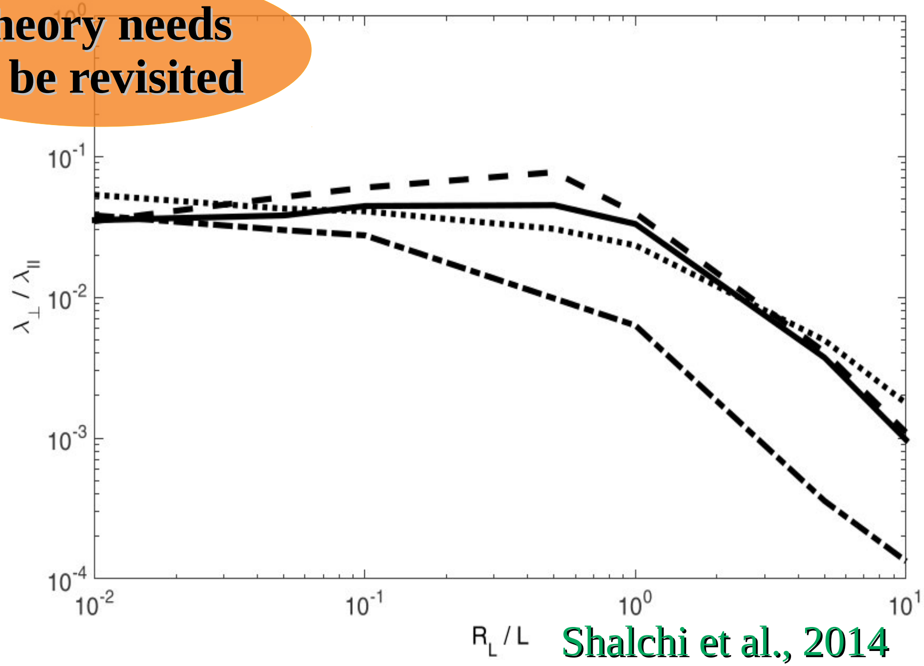

Shalchi et al., 2014
Hussein et al., 2015

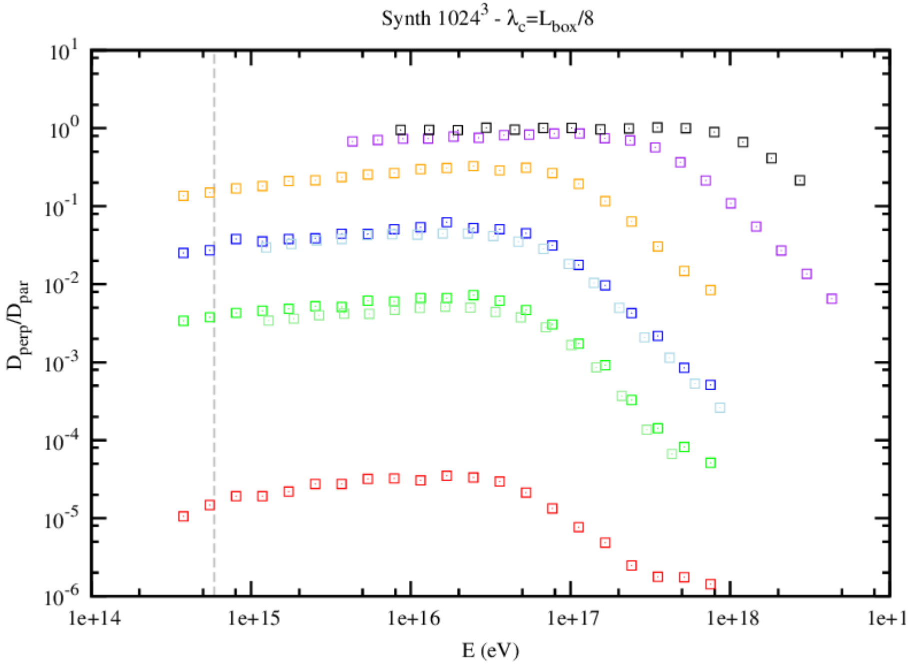

Case with B_0: theoretical needs

NLGC as well as further “universal” theories predict that **$D_{||}$ and D_{perp} are parallel**.

Numerical simulations were actually indicating a **different behavior**!

We can provide now a better evidence of such behavior (grid up to 2048^3)

Theory needs to be revisited

NLGC Main Assumptions:

- **4th order correlator** $\langle v_z(t)\delta B_x(t)v_z(0)\delta B_x^*(0)\rangle \longrightarrow \langle v_z(t)v_z(0)\rangle\,\langle \delta B_x(t)\delta B_x^*(0)\rangle$

Matthaeus et al., APJ 2003

Case with B_0: theoretical needs

NLGC as well as further "universal" theories predict that **$D_{||}$ and D_{perp} are parallel**.

Numerical simulations were actually indicating a **different behavior**!

We can provide now a better evidence of such behavior (grid up to 2048^3)

Theory needs to be revisited

NLGC Main Assumptions:

- **4th order correlator** $\langle v_z(t)\delta B_x(t) v_z(0)\delta B_x^*(0)\rangle \longrightarrow \langle v_z(t)v_z(0)\rangle \langle \delta B_x(t)\delta B_x^*(0)\rangle$
- **Velocity Correlator** $V_{zz}(t) = \langle v_z(t)v_z(0)\rangle = \frac{v^2}{3} e^{-vt/\lambda_{\parallel}}$

Matthaeus et al., APJ 2003

Case with B_0: theoretical needs

NLGC as well as further "universal" theories predict that **$D_{||}$ and D_{perp} are parallel**.

Numerical simulations were actually indicating a **different behavior**!

We can provide now a better evidence of such behavior (grid up to 2048^3)

Theory needs to be revisited

NLGC Main Assumptions:

- **4th order correlator** $$\langle v_z(t)\delta B_x(t)v_z(0)\delta B_x^*(0)\rangle \longrightarrow \langle v_z(t)v_z(0)\rangle \langle \delta B_x(t)\delta B_x^*(0)\rangle$$
- **Velocity Correlator** $$V_{zz}(t) = \langle v_z(t)v_z(0)\rangle = \frac{v^2}{3}\, \mathrm{e}^{-vt/\lambda_{\|}}$$
- **Corrsin hypothesis (+ Hom. Turb.)** $$R_{xx}(t) = \int \mathrm{d}^3k\ \langle \delta B_x(\mathbf{k},t)\delta B_x^*(\mathbf{k},0)\,\mathrm{e}^{i\mathbf{k}\cdot\Delta\mathbf{x}}\rangle,$$ $$R_{xx}(t) = \int \mathrm{d}^3k\ P_{xx}(\mathbf{k},t)\langle \mathrm{e}^{i\mathbf{k}\cdot\mathbf{x}}\rangle$$

Matthaeus et al., APJ 2003

Case with B_0: theoretical needs

NLGC as well as further "universal" theories predict that **$D_{||}$ and D_{perp} are parallel**.

Numerical simulations were actually indicating a **different behavior**!

We can provide now a better evidence of such behavior (grid up to 2048^3)

Theory needs to be revisited

$$\kappa_{xx} = \frac{a^2 v^2}{3B_0^2} \int \frac{S_{xx}(\boldsymbol{k}) dk_x\, dk_y\, dk_{\|}}{\frac{v}{\lambda_{\|}} + (k_x^2 + k_y^2)\kappa_{xx} + k_{\|}^2 \kappa_{zz} + \gamma(\boldsymbol{k})}$$

NLGC Main Assumptions:

- **4th order correlator** $\langle v_z(t)\delta B_x(t) v_z(0)\delta B_x^*(0)\rangle \rightarrow \langle v_z(t) v_z(0)\rangle \langle \delta B_x(t)\delta B_x^*(0)\rangle$
- **Velocity Correlator** $V_{zz}(t) = \langle v_z(t) v_z(0)\rangle = \frac{v^2}{3} e^{-vt/\lambda_{\|}}$
- **Corrsin hypothesis (+ Hom. Turb.)**

$$R_{xx}(t) = \int d^3k \, \langle \delta B_x(\mathbf{k}, t)\delta B_x^*(\mathbf{k}, 0)\, e^{i\mathbf{k}\cdot\Delta\mathbf{x}}\rangle,$$

$$R_{xx}(t) = \int d^3k \; P_{xx}(\mathbf{k}, t) \langle e^{i\mathbf{k}\cdot\mathbf{x}}\rangle$$

- **Closure (diffusive, ballistic etc) for the charact. function**

Matthaeus et al., APJ 2003

Conclusions and perspective

- **Preliminary numerical results concerning the CRs tranport in a prescribed (synthetic) turbulent magnetic field**
  - Numerical tools are quite robust (different implementations, different methods)
  - Improved dynamical range allows to analyze CRs diffusion in the inertial range of turbulence for more than an order of magnitude of energy
  - Numerical results confirm the validity of the Subedi's theory for $B_0=0$
  - When B_0 is present, D_{perp} and $D_{||}$ show different slopes with respect to particle energy
- **Perspectives:**
  - Theories need to be revisited since they predict the same energy dependencs of D_{perp} and $D_{||}$
  - Comparison with the results obtained with magnetic fields generated through MHD simulation may shed light on the role of **intermittency** and **particles acceleration**